International Journal on Magnetic Particle Imaging
Vol 12, No 1, Suppl 1, Article ID 2603037, 3 Pages

Infinite Science Publishing

Proceedings Article

Deep image prior for alternating direction method of multipliers reconstruction of experimental magnetic particle imaging data

Antonis Nikolakis [a,b,*] · George A. Kastis [a] · Jing Zhong [c] · Nikolaos Dikaios [a]

[a] Mathematics Research Center, Academy of Athens, Greece
[b] Department of Physics, National & Kapodistrian University of Athens, Greece
[c] School of Instrumentation and Opto-Electronic Engineering, Beihang University, Beijing, China
[*] Corresponding author, email: tonynikpl@phys.uoa.gr

Abstract

This work presents an on-the-fly training Deep Image Prior (DIP) integrated into an Alternating Direction Method of Multipliers (ADMM) algorithm for Magnetic Particle Imaging (MPI) system-matrix reconstruction. Experimental data results indicate competitive quality and robustness, supporting the approach as a practical alternative to classical Tikhonov.

I. Introduction

Magnetic Particle Imaging (MPI) detects superparamagnetic nanoparticles directly by measuring the voltage induced on receive coils as their magnetization changes under a tailored magnetic field sequence [1]. Reconstructing the nanoparticle concentration from these signals is a challenging inverse problem. The encoding is ill-conditioned; measurements contain noise and interference; and trajectory design (type, density etc.) can limit the recoverable detail. This inverse problem is typically ill-posed and noise-sensitive [2]. This work proposes a novel approach in which a Deep Image Prior (DIP) [3] regularizes the ill-posed inverse problem, while an Alternating Direction Method of Multipliers (ADMM) decouples the data fidelity and prior enforcement steps, enabling robust handling of noise and ill-conditioning.

II. Materials and Methods

Given a complex system matrix $A \in \mathbb{C}^{M\times N}$ and measured data $b \in \mathbb{C}^M$, the task is to estimate the nanoparticle concentration image $c \in \mathbb{C}^N$. Reconstruction is posed as an inverse problem: $\|Ac - b\|_2^2 \le \varepsilon, \quad c \ge 0$. An ADMM scheme enforces data consistency and nonnegativity while letting individual priors act on their own copy of the image through proximal steps. The implemented ADMM algorithm utilizes an ℓ_1 prior (sparsity) and a total variation (TV) prior (edge–preserving smoothing). A similar ADMM implementation can be found in [4]. This work introduces a training-free DIP as a prior into the ADMM algorithm. For each prior $p \in \{\ell_1, \mathrm{TV}, \mathrm{DIP}\}$, ADMM maintains a pair $(z^{(p)}, u^{(p)})$ that enforces the constraint $c = z^{(p)}$. Intuitively, $z^{(p)}$ is the version of the image after applying prior p, and $u^{(p)}$ accumulates the current disagreement between c and that version.

The proximal operator is realized with a compact, untrained UNet f_θ that receives a *fixed* Gaussian noise tensor as input with a small normalized fraction of the current iterate $\mathbf{t}^{(\mathrm{DIP})}$ added for stability. At each outer ADMM iteration (algorithm 1), f_θ is optimized for a limited number of steps to reproduce the current target image $\mathbf{t}^{(\mathrm{DIP})} = \mathbf{c} + \mathbf{u}^{(\mathrm{DIP})}$ in normalized intensity space. An early stopping strategy selects the iteration of maximum

Algorithm 1 One outer Hybrid ADMM iteration with data constraint, ℓ_1, and TV *or* DIP prior (plus nonnegativity)

Require: System matrix A, measurements b, tolerance ε, weights α_1, α_2, penalty μ, relaxation $\rho \in (0,1]$.

1: Solve for c (CG):
Solve

$$\left(A^H A + 3I\right) c = A^H\left(z^{(\text{data})} - u^{(\text{data})}\right) + \sum_{p\in\{\ell_1,2,\text{nn}\}} \left(z^{(p)} - u^{(p)}\right).$$

using Conjugate Gradients.

2: Proximal / projection updates for z:
Data fidelity: $z^{(\text{data})}_{\text{new}} \leftarrow \text{proj}_{\|\cdot - b\|_2 \le \varepsilon}\left(Ac + u^{(\text{data})}\right)$.
ℓ_1: $z^{(\ell_1)}_{\text{new}} \leftarrow \text{soft}\left(c + u^{(\ell_1)}, \alpha_1/\mu\right)$.
Nonnegativity: $z^{(\text{nn})}_{\text{new}} \leftarrow \max\left(c + u^{(\text{nn})}, 0\right)$.
*Prior split $z^{(2)}$ (2: TV **or** DIP):*
Set $t^{(2)} \leftarrow \text{reshape}\left(c + u^{(2)}\right)$ and $w \leftarrow \alpha_2/\mu$.
If TV is used: $z^{(2)}_{\text{new}} \leftarrow \text{prox}_{\text{TV}}\left(t^{(2)}; w\right)$ (isotropic TV prox).
If DIP is used: $z^{(2)}_{\text{new}} \leftarrow \text{DIP}\left(t^{(2)}; w\right)$
Normalize target: $\tilde{t} \leftarrow (t^{(2)} - \text{mean}(t^{(2)}))/(\text{std}(t^{(2)}) + \epsilon)$.
Compute DIP weight and clip: $w_{\text{safe}} \leftarrow \text{clip}(w, 0.05, 0.5)$.
Fixed DIP input: initialize a noise tensor $z_0 \sim 0.05\,\mathcal{N}(0,1)$, constant for all ADMM iterations.
Train a UNet f_θ for a fixed number of Adam steps to fit $\tilde{t}$ from z_0:

$$\theta \leftarrow \arg\min_\theta \frac{1}{w_{\text{safe}}} \left\| f_\theta(z_0) - \tilde{t} \right\|_2^2.$$

3: Relaxation for stability:
$z^{(p)} \leftarrow \rho\, z^{(p)}_{\text{new}} + (1-\rho)\, z^{(p)}, \quad p \in \{\text{data}, \ell_1, 2, \text{nn}\}$.

4: Dual updates for u (scaled ADMM form):
$u^{(\text{data})} \leftarrow u^{(\text{data})} + (Ac - z^{(\text{data})})$.
$u^{(p)} \leftarrow u^{(p)} + (c - z^{(p)}), \quad p \in \{\ell_1, 2, \text{nn}\}$.

5: μ adaptation (periodic residual balancing):
Every few iterations, adjust μ based on primal/dual imbalance. If μ changes, rescale the scaled duals: $u^{(p)} \leftarrow (\mu_{\text{old}}/\mu)\, u^{(p)}$ for all splits.

edge activity. The resulting output is denormalized and smoothed with a Gaussian filter for stability. The same network parameters are retained across outer ADMM iterations. Finally, $\mathbf{z}^{(\text{DIP})}$ is clamped to $[0,1]$ before being used in the next ADMM update to maintain normalization consistency.

To assess evenness of the reconstructed image, a uniformity score based on global variation is used: $U = \exp(-\kappa\, \text{std}(c))$ where c is the reconstructed image, std is the global standard deviation and κ is a fixed scaling factor that forces values in the $[0,1]$ range.

III. Results

The ADMM schemes were observed to be prone to hotspot formation, which can dominate the dynamic range and effectively obscure lower-intensity regions. To suppress that, median filtered reconstruction results of experimental data [5] are shown in figure 1. On the median-filtered images the uniformity metric gives: $U_{Tik} = 0.913$, $U_{ADMM-TV} = 0.909$, and $U_{ADMM-DIP} = 0.916$, with DIP being slightly higher.

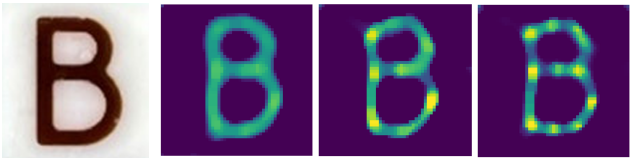

(a) Phantom **(b)** Tikhonov **(c)** ADMM-TV **(d)** ADMM-DIP

Figure 1: Phantom and median filtered reconstructions.

IV. Discussion

ADMM with or without a deep prior is an effective reconstruction approach for MPI [4]. The split formulation delivers stable convergence and produces images with clean backgrounds and delineated structures. The ℓ_1 suppresses small isolated coefficients (promoting sparsity), the TV removes oscillatory noise while preserving edges and the DIP further aids with edge preservation.

Acknowledgments

This work was funded by the Sectoral Development Program (SDP 5223471) of the Ministry of Education, Religious Affairs and Sports, through the National Development Program (NDP) 2021-25. Furthermore, this publication is based upon work from COST Action Next Generation Magnetic Particle Imaging (NexMPI) - CA23132 supported by COST (European Cooperation in Science and Technology).

Author's statement

Conflict of interest: Authors state no conflict of interest.

References

[1] B. Gleich and J. Weizenecker. Tomographic imaging using the nonlinear response of magnetic particles. *Nature*, 435(7046):1214–1217, 2005, doi:10.1038/nature03808.

[2] L. Yin, W. Li, Y. Du, K. Wang, Z. Liu, H. Hui, and J. Tian. Recent developments of the reconstruction in magnetic particle imaging. *Visual computing for industry, biomedicine, and art*, 5(1):24, 2022.

[3] S. Dittmer, T. Kluth, M. T. R. Henriksen, and P. Maass, Deep image prior for 3d magnetic particle imaging: A quantitative comparison of regularization techniques on open mpi dataset, 2020. arXiv: 2007.01593.

[4] S. Ilbey, C. B. Top, A. Güngör, T. Çukur, E. U. Saritas, and H. E. Güven. Comparison of system-matrix-based and projection-based reconstructions for field free line magnetic particle imaging. *International Journal on Magnetic Particle Imaging IJMPI*, 3(1), 2017.

[5] R. Zhang, S. Sun, S. Sun, M. Meribout, L. Xu, and J. Zhong. Mixing-space magnetic particle imaging. *IEEE Transactions on Instrumentation and Measurement*, 74:1–9, 2025, doi:10.1109/TIM.2024.3500075.

